Evaluation of WRF performance for the analysis of surface wind speeds over various Greek regions

Nikolaos Christakis and Theodoros Katsaounis and Georgios Kossioris and Michael Plexousakis

Evaluation of WRF performance for the analysis of surface wind speeds over various Greek regions

Christakis N.[1], Katsaounis Th.[2], Kossioris G.[2], Plexousakis, M.[2]*

1 Department of Physics, University of Crete, and Institute of Applied and Computational Mathematics, FO.R.T.H., Heraklion

2 Department of Mathematics and Applied Mathematics, University of Crete, and Institute of Applied and Computational Mathematics, FO.R.T.H., Heraklion

*corresponding author e-mail: plex@tem.uoc.gr

Abstract In this study we analyze the surface wind variability over selected areas of the Greek territory by comparing a 3-km-spatial resolution simulation performed with the Weather Research and Forecasting (WRF) model for the summer months of 2013 with actual surface measurements. Daily 36hrs runs at 12 UTC were driven by FNL (1°× 1°) data for the period of 11 July 2013 to 17 July 2013. Various verification statistics, such as bias, RMSE and DACC for wind speed and direction were used to gauge the mesoscale model performance.

1 Introduction

In this paper, we analyze the performance of the WRF model in estimating the near-surface wind variability over selected areas of Greece. Such an analysis is mostly missing for Greece, while being of utmost importance for the growing wind power industry and civil protection agencies, due the increased occurrence of extreme weather events. The sensitivity of the WRF model for several parametrizations is measured against ten wind-measuring stations consisting of 30 m masts equipped with vane anemometers. We chose to simulate a typical summer period, 11-17 July 2013, characterized by Etesian winds of moderate to strong north or north-easterly winds.

The 11-17 July 2013 event, was typically characterized by Etesian winds. They are northern sector winds blowing over the Aegean Sea during summer and early autumn. They are mainly north-easterly in the northern Aegean, northerly in the central and southern Aegean, and tend to become north-westerly near the south-western Turkish coasts, see e.g. (Kotroni et al., 2001). The Etesians are the consequence of a high-pressure center in the central and south-east Europe and a low-pressure system that extends from Turkey to northwest India, see e.g. (Reiter

et al., 1980), (Metaxas and Bartzokas, 1994). According to the simulations (surface plots not shown here), during the event, a high pressure system of 1015-1020 hPa was prevailing in central and eastern Europe. A low-pressure center of 990-995 hPa was extended south-east of Turkey reaching Persian Gulf.

The remaining of the paper is organized as follows: Section 2 describes the acquisition of observational data used in the analysis and the set up of the simulations with the WRF mesoscale model. Section 3 contains an analysis of the mesoscale model performance using various verification statistics. Our findings are summarized in Section 4.

2 Data and Methodology

A total of 10 observational sites was used in this investigation, with wind speed and direction measurements recorded at 20m, 28m and 30m above ground level. All simulations reported here in were performed with WRF version 3.4 (Skamarock et al., 2005). The locations of the observation (surface) stations and their codes are shown in Fig. 1. This observational network provides good spatial coverage, sampling many important locations that are representative of the topographic characteristics of Greece.

Fig.1 Locations of the observational sites together with their codes.

2.1 Data

Wind speed and wind direction were recorded by vane anemometers, placed on 30 m masts located at the observation stations mentioned above, for the week between 11 and 17 July 2013. The masts were deployed as part of the research

project AKAIPRO, see (AKAIPRO, 2011). The 10 min average wind speed and wind direction at 28 m above ground level were used for comparison with the WRF simulations. In turn, the WRF-simulated wind speed and wind direction were estimated at 28m by interpolation, specifically by using NCL's wrf_interp_3d function.

2.2 Methodology

Numerical experiments were conducted to simulate the aforementioned event using WRF with one-way nested domains. The initial and boundary conditions are derived from the National Centers for Environmental Prediction (NCEP) model analysis by WRF preprocessing. An improved representation of topography with 60 m × 60 m spatial resolution (Abrams et al., 2010, Toutin, 2008) and an updated land-use dataset with 24 land-use categories from the U.S. Geological Survey (USGS) were used in order to ensure more accurate surface conditions. The Noah land surface model was used.

Three one-way nested domains with horizontal grid resolutions of 27 km, 9 km and 3km, respectively were specified. The innermost domain covers the entire Greek territory while the outermost domain contains most of Europe. All modeling domains had 50 layers in the vertical dimension, with the model top being set at 50 hPa. The Kain-Fritsch scheme (Kain, 2004) was used for parametrizing cumulus convection. Shortwave radiation processes were handled using a cloud radiation scheme (Dudhia, 1989) and the Rapid Radiative Transfer Model (RRTM) scheme (Mlawer E.J. et al., 1997) was applied for longwave radiation processes. A total of nine different parametrizations, referred to in the sequel as P1 to P9, using three different microphysics options and three different planetary boundary layer schemes were used in simulating the weather event in 11-17 July 2013. Parametrizations P1 to P3 used the simple WRF single-moment six-class scheme for micro-physics (Dudhia et al., 2008; Hong et al., 2004; Lin et al., 1983). Parametrizations P4 to P6 used the Ferrier micro-physics option (Ferrier et al., 2002) and P7 to P9 used the New scheme (Thompson et al., 2004). The PBL scheme used in parametrizations P1, P4 and P7 was the Yonsei University scheme (Hong et al., 2006). Parametrizations P2, P5 and P8 used the Mellor-Yamada-Janjic scheme (Janjic, 1994), while P3, P6 and P9 used the MYNN3 Nakanishi and Niino scheme (Nakanishi and Niino, 2006).

The validation of the WRF model physics parametrizations is done by computing various statistics for both the wind speed and direction. Namely, we use four different metrics. The wind speeds are validated using the standard Bias and RMSE measures and their relative counterparts, while for the wind direction we use the relative Bias and the DACC statistics, see (Santos-Alamillos et al., 2013). Let m_i and o_i denote the modeled and observed values of wind speed, respectively. The first metric we use is the Mean Error or Bias which measures the overall

overestimation or underestimation of modeled wind speed values and it is defined by

$$BIAS = \frac{1}{N}\sum_{i=1}^{N}(m_i - o_i) \quad \text{and} \quad \textbf{Relative } BIAS = \frac{BIAS}{O_{avg}} \times 100$$

where $O_{avg} = \frac{1}{N}\sum_{i=1}^{N} o_i$ with N the number of records. The second metric we use is the Root Mean Square Error (RMSE) between the modeled and observed values and measures the amount of scatter of the wind speed errors:

$$RMSE^2 = \frac{1}{N}\sum_{i=1}^{N}(m_i - o_i)^2 \quad \text{and} \quad \textbf{Relative } RMSE = \frac{RMSE}{O_{avg}} \times 100$$

To measure the directional accuracy of the wind, besides the relative BIAS metic, we also adopted the *DACC* metric. For any two angles α and β the circular distance is defined as $\Delta\theta(\alpha,\beta)=\min|\alpha-\beta, 360^o-(\alpha-\beta)|$.
Then the DACC metric measures the percentage of times in which the circular distance between modeled and observed wind directions is lower than a threshold, chosen as 30°:

$$DACC = \frac{\sum_{i=1}^{N} \begin{cases} 1, & \text{if } 0 \le \Delta\theta_i \le 30 \\ 0, & \text{otherwise} \end{cases}}{N} \times 100$$

3 Results

We divided the ten observation sites in three groups, each group representing a geographical region of Greece and with the sited in each group being of related meteorological characteristics for the event under investigation, see Fig. 1. The group labeled Northern Greece, consisted of the stations Evzonoi (eyz), Kavala (kav), Loutro (ltr) and Ptolemaida (ptl). The group Western Greece consisted of the sites Delvinaki (dlv), Patra (ptr) and Pylos (pyl). Finally, the group labeled South-Central Greece consisted of the sites Kissamos (kis), Toplou (tpl) and Volos (vol). Figure 2 shows the relative BIAS and the relative RMSE of the wind speed measured at 28 m above ground level, as well as, the relative BIAS and the DACC for the wind direction. The relative wind speed bias is quite low, under 5%, for all sites in this group with the exception of the station of Pylos (pyl) where it is under

10%. WRF underestimates the wind speed at the near-coastal stations of Patra and Pylos while it overestimates the wind speed at the mountainous station of Delvinaki (dlv). All stations are characterized by a positive relative BIAS for the wind direction indicating a clock-wise deviation of the simulated wind. The wind direction DACC indices range between 40% and 60% with that of Pylos being above 50%. The relative RMSE scores for the wind speed are between 35% and 60% with Patras and Pylos being almost below 40%, consistently for all nine parametrizations. The high relative RMSE score for the Delvinaki site may be attributed to the high elevation and terrain complexity.

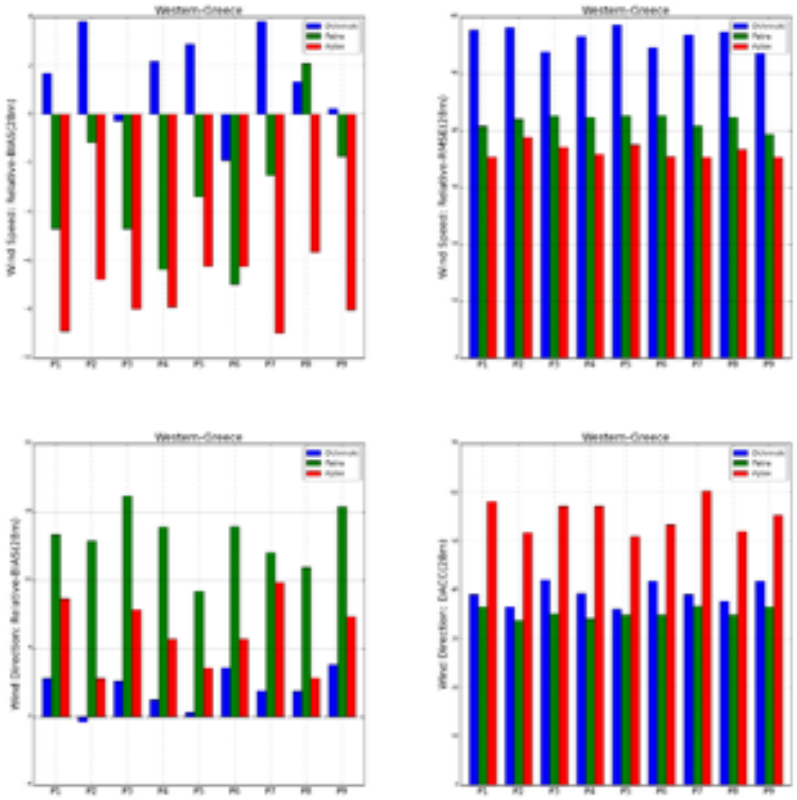

Fig. 2. Relative BIAS and relative RMSE of the wind speed measured at 28 m above ground level (top panel), as well as, relative BIAS and DACC for the wind direction at 28 m above ground level (bottom panel) for the sites in the group Western Greece.

Figure 3 shows the relative BIAS and the relative RMSE of the wind speed measured at 28 m above ground level, as well as, the relative BIAS and the DACC for the wind direction also at 28 m above ground level, for the sites in the group Northern Greece. The relative wind speed bias is quite low, under 5%, for almost all parametrizations and sites in this group. All sites are characterized by a

negative relative BIAS for the wind direction, except the Kavala site. In addition, all sites except Loutro have a very small relative BIAS, less than 5% in absolute value. The relative BIAS for the Loutro site is approximately -20%, consistently across all parametrizations. The wind direction DACC index in quite good for the Evzonoi site, almost acceptable for Loutro and poor for the Kavala and Ptolemaida sites. The relative RMSE scores for the wind speed are between 30% and 65% with Loutro and Evzonoi being below 40%, consistently for all nine parametrizations.

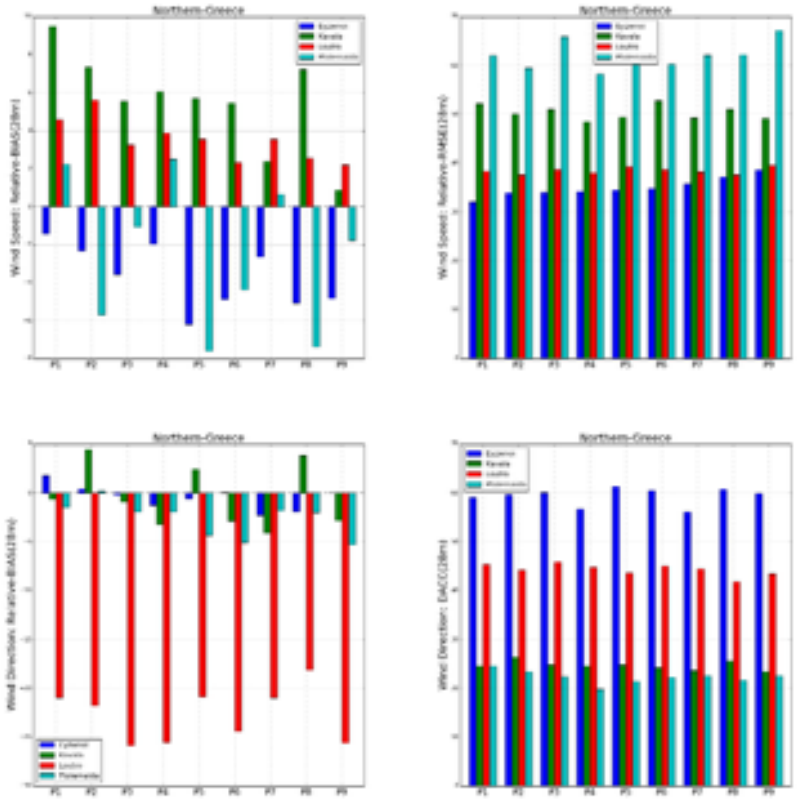

Fig. 3. As in Fig 2. but for the sites of the group Northern Greece.

Figure 4 shows the relative BIAS and the relative RMSE of the wind speed measured at 28 m above ground level, as well as, the relative BIAS and the DACC for the wind direction also at 28 m above ground level for the sites in the group South-Central Greece. The relative wind speed bias is low, under 5%, for all sites in this group with exception of the station Kissamos (kis) where it is under 15%. The relative BIAS for the wind direction for the sites of Toplou and Kissamos is quite low, around 5%, but the Volos site shows a score between -10% and -18%. The wind direction DACC index for the Toplou site is extremely good. Figure 5

shows the energy wind rose for the Toplou site for the parametrization P9, where the excellent agreement of the sectorial-wise distribution is clearly evident. Figure 6 shows the energy wind rose for the Kissamos site for the parametrization P9. Although WRF captures the tendency of the prevailing NE or ENE wind direction, it does not capture as accurately the sectorial-wise distribution and misses completely a small easterly sector, see Fig. 6. The relative RMSE scores for the wind speed in the Toplou station are around 10% for all parametrizations, while Volos and Kissamos show scores around 40% and 30%, respectively.

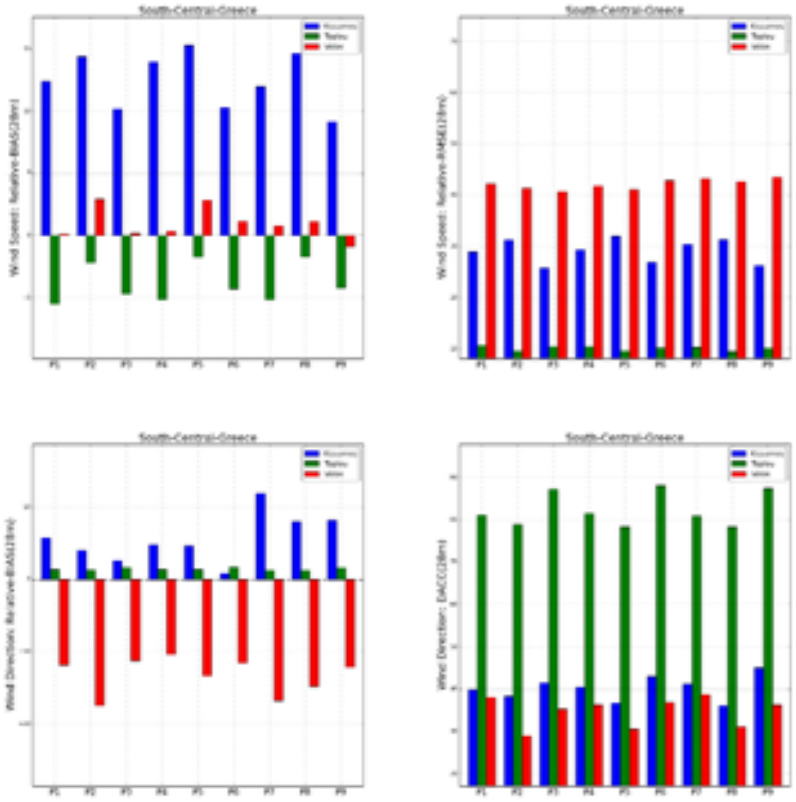

Fig. 4. As in Fig 2. but for the sites in the group South-Central Greece.

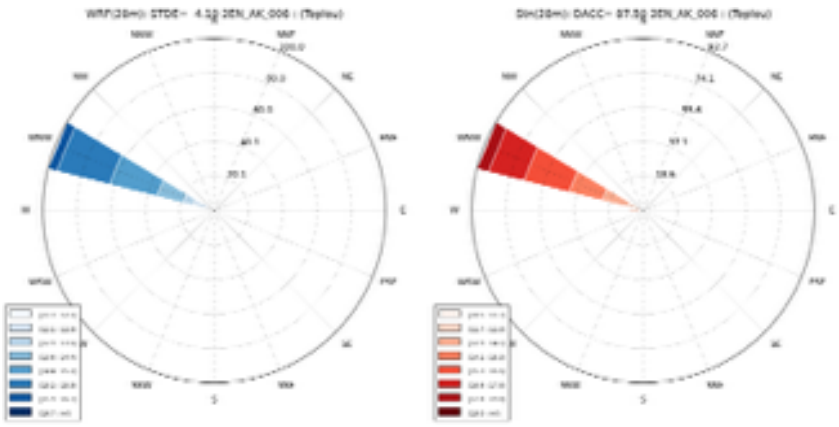

Fig. 5. Energy wind roses for the Toplou site for the parametrization P9. WRF-simulated wind at left, observational data at right.

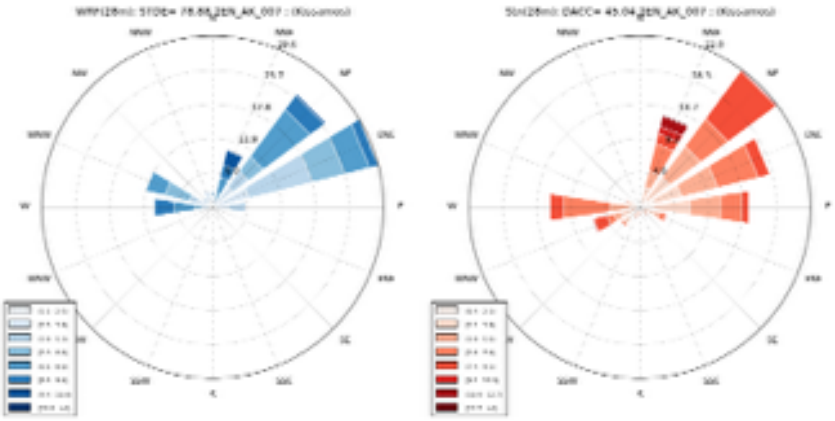

Fig. 6. Energy wind rose for the Kissamos site for the parametrization P9. WRF-simulated wind at left, observational data at right.

4 Conclusions

Regarding wind speed relative bias, parametrizations P9 and P7 give the lowest values for the stations of the group Northern Greece. P9 and P8 give the lowest relative bias in stations in the group Western Greece with P9 performing quite well also in the South-Central Greece group (see Fig. 4). In all the above parametrizations the microphysics option is Thompson with PBL parametrization NYMM3 for P9 (see Fig. 2, 3, and 4). Regarding relative RMSE, no parametrization has a clear overall better performance. Regarding the performance of parametrizations for wind direction, P2 and P8 perform quite well in all geographic regions.

Acknowledgement. G. Kossioris, Th. Katsaounis and M. Plexousakis have been partially supported by the European Union Seventh Framework Programme (FP7-REGPOT-2009-1) under the Grant Agreement no. 245749 (Archimedes Center for Modeling, Analysis and Computation, University of Crete, Greece).

References

Abrams M, Bailey B, Tsu H, Hato M (2010) The ASTER Global DEM. Photogramm Eng Remote Sens 76:344–348.

AKAIPRO, Study of extreme weather phenomena in local regions and their impact to civil protection. Research Program “SYNERGASIA”, Greek Secretariat of Research and Technology, 2011-2013. http://idarkstar.tem.uoc.gr/~plex/newakaipro.

Carvalho D, Rocha A, Gomez-Gesteira M, Santos C (2012): A sensitivity study of the WRF model in wind simulation for an area of high wind energy, Environmental Modelling & Software, 33:23-34.

Dudhia, J., 1989: Numerical study of convection observed during the winter monsoon experiment using a mesoscale two-dimensional model, J. Atmos. Sci., 46, 3077–3107.

Ferrier, B. S., Y. Lin, T. Black, E. Rogers, and G. DiMego, 2002: Implementation of a new grid-scale cloud and precipitation scheme in the NCEP Eta model. Preprints, 15th Conference on Numerical Weather Prediction, San Antonio, TX, Amer. Meteor. Soc., 280-283.

Hong, S.-Y., J. Dudhia, and S.-H. Chen, 2004: A Revised Approach to Ice Microphysical Processes for the Bulk Parameterization of Clouds and Precipitation, Mon. Wea. Rev., 132, 103–120.

Janjic, Z. I., 1994: The step–mountain eta coordinate model: further developments of the convection, viscous sublayer and turbulence closure schemes. Mon. Wea. Rev, 122, 927–945.

Kain J. S., 2004: The Kain–Fritsch Convective Parameterization: An Update. Journal of Applied Meteorology, 43, No. 1, pp. 170–181

Kotroni V, Lagouvardos K, Lalas D (2001) The effect of the island of Crete on the Etesian winds over the Aegean Sea. Q J R Meteorol Soc 127:1917–1937.

Lin, Y.-L., R. D. Farley, and H. D. Orville, 1983: Bulk parameterization of the snow field in a cloud model. J. Climate Appl. Meteor., 22, 1065–1092.

Metaxas DA, Bartzokas A (1994) Pressure covariability over the Atlantic, Europe and N. Africa. Application: Centers of Action for Temperature, Winter Precipitation and Summer Winds in Athens, Greece. Theor. Appl. Climatol. 49:9–18.

Mlawer, E. J., S. J. Taubman, P. D. Brown, M. J. Iacono, and S. A. Clough, 1997 Radiative transfer for inhomogeneous atmosphere: RRTM, a validated correlated-k model for the longwave. J. Geophys. Res., 102 (D14), 16663–16682.

Nakanishi N., and Niino H. (2006): An improved Mellor-Yamada Level-3 model: Its numerical stability and Application to a regional prediction of Advection fog. Boundary-layer Met., 119, 397:407.

Reiter E.R, Brody L.R., Nestor M.J.R. (1985): Handbook for forecasters in the Mediterranean, Monterey Calif. : Environment Prediction Research Facility, Naval Postgraduate School, 1975-1980.

Santos-Alamillos F.J., Pozo-Vazquez D, Ruiz-Arias J.A, Lara-Fanego V, Tovar-Pescador J. (2013): Analysis of WRF model wind estimate sensitivity to physics parametrization choice and terrain representation in Andalusia (Southern Spain), Journal of Applied Meteorology and Climatology, 52:1592:1609

Skamarock, W. C., J. B. Klemp, J. Dudhia, D. O. Gill, D. M. Barker, W. Wang, and J. G. Powers, 2005: A description of the Advanced Research WRF Version 3. NCAR Tech Notes-475+STR, 113pp.

Thompson, G., R. M. Rasmussen, and K. Manning, 2004: Explicit forecasts of winter

precipitation using an improved bulk microphysics scheme. Part I: Description and sensitivity analysis. Mon. Wea. Rev., 132, 519–542.

Toutin T (2008) ASTER DEMs for geomatic and geoscientific applications: a review. Int J Remote Sens 29:1855–1875.